SEMARAK ILMU PUBLISHING

Journal of Advanced Research in Applied Mechanics

Journal homepage:
https://semarakilmu.com.my/journals/index.php/appl_mech/index
ISSN: 2289-7895

Evaluation of Volume to Area Ratio to Aluminum Alloy Microstructure

Mohd Nasuha Ab Halim[1], Mohd Rashidi Maarof[1,2,*], Mohamed Reza Zalani[1], Asnul Hadi Ahmad[1]

[1] Manufacturing Research Focus Group (MFG), Faculty of Mechanical and Automotive Engineering Technology, Universiti Malaysia Pahang (UMP), 26600 Pekan, Pahang, Malaysia
[2] Automotive Engineering Centre, Universiti Malaysia Pahang (UMP), 26600 Pekan, Pahang, Malaysia

ARTICLE INFO

Article history:
Received 30 October 2024
Received in revised form 1 December 2024
Accepted 8 December 2024
Available online 30 December 2024

Keywords:
Metal casting; alumnium-silicon; grain; V/A ratio

ABSTRACT

The volume to area ratio of the cavity dimension in aluminum alloy is the foundation of this study. Afterwards, the metal casting product's hardness and grain size at various points were compared. A hardness test and optical microstructure observation were part of the experiment. The findings indicate a correlation between the microstructure and the volume to area ratio. The harder and stronger the material, the smaller the grain size and the higher the ratio.

1. Introduction

An element known as a pump shaft attachment or pump coupling connects the rotating pump shaft to the driven shaft, allowing the engine to supply power to the pump effectively. When the pump is closely linked, there is no need for a separate connection because the engine is mounted directly on a single shaft. Although close-coupled pumps are small and reasonably priced, their common rolling stocks are under more stress, and the motor's size is typically restricted, making them less suitable for heavy duty, high strength, and continuous use. It compensates for shaft misalignment, guards against surpluses, and absorbs shock charges from one shaft to another. There are several different types of pump connectivity, such as flange, jaw, fluid, flexible, and rigid couplings.

When two shafts are exactly parallel, a rigid coupling is utilized. It is accurately alignable. In motion control applications, the jaw coupling is then used for general power transfer. The jaw coupling's goal is to transfer torque while minimizing system vibration and misalignment. Furthermore, the flange coupling is made up of two flanges that are connected at the ends of every shaft. Bolts and nuts hold both flanges in place. The pressurized pipe systems are where these couplings are most commonly found.

* *Corresponding author.*
E-mail address: mrashidi@umpsa.edu.my

https://doi.org/10.37934/aram.130.1.180189

This part is subjected to bending, compression, and inertial forces in addition to tensile strength. Because of its durability, cost of production, and manufacturing process, the material used to make the pump coupling must be carefully chosen to allow it to withstand all of this force. Since there is less load during torque transfer, there is a chance that the common iron coupling will be replaced with aluminum. The reason for this is that aluminum can be cast at a relatively lower melting temperature and does not harden as much during machining.

In comparison to other materials, aluminum is stiffer, lighter, more stable, and has a higher level of safety. Furthermore ductile, affordable, and resistant to corrosion at low temperatures are alloys made of aluminum. The density of aluminum is 2.7 g/cm3, which is approximately one-third that of steel (7.83 g/cm3) [1]. About 480 pounds of steel and 160 pounds of aluminum were found per cubic foot. This small weight, when paired with the high strength of certain aluminum combinations (which surpass structural stain), enables the design and construction of sturdy, lightweight structures.

Martin [2] claims that even though aluminum alloys have a low melting point, during solidification, they undergo significant shrinkage. To ensure precise dimensions in the final product, shrinkage of 3.5 to 8.5 percent is possible and needs to be taken into account during the mold design process.

Aluminum-silicon alloys are typically used in the majority of aluminum casting alloy applications. Castings made with this coarse eutectic are brittle, likely due to the brittle nature of silicone particles. Refining the eutectic can be achieved through modification (adding metallic sodium or sodium salts to the melt before pouring) or faster cooling (as in permanent mold casting) to improve the mechanical properties of the casting [3]. The adjustment is not necessary when the silicon concentration of aluminum is 8% because there is enough silicon in the initial aluminum phase to provide suitable ductility. This alloying stage is primarily managed during the melting process.

Nevertheless, shrinkage factor can occur during the silicon casting process of aluminum alloys [4]. When there is not enough feed metal to offset shrinkage as the metal solidifies, shrinkage defects arise. Shrinkage defects come in two flavors: open shrinkage defects and closed shrinkage defects. Air compensates during the shrinkage cavity formation process because open shrinkage defects are exposed to the atmosphere. There are two categories of open-air defects: pipes and caved surfaces. Caved surfaces are shallow cavities that form across the surface of the casting, whereas pipes form on the surface and burrow into the casting. Shrinkage porosity, another term for closed shrinkage defects, is a feature of the casting [5].

Hot spots are distinct liquid pools that form inside of solidified metal and are one of the criteria used to calculate shrinkage factor. The shrinkage defect usually shows up at the top of the heated areas. Closed shrinkage defects can be brought on by impurities and dissolved gas since they need a nucleation point. According to Ingle and Sorte [6], the defects are divided into two categories: macroporosity and microporosity (or microshrinkage), with macroporosity being visible to the unaided eye and microporosity not.

As a result of the molten metal needed for solidification shrinkage not being replenished, shrinkage happens when a particular section of the solidified material forms a closed loop, leading to the formation of a cavity. As previously mentioned, the surface can be entrained by simply contracting [7]. However, because the surface turbulence event is typically chaotic, pockets of air may inadvertently be trapped by chance creases and folds at random locations in the double film if the surface is disturbed more severely, as is common during the pouring of liquid metals. Porosity scattering in castings as a result seems to be almost always caused by entrained air pockets [8].

Shrinkage cavities that resulted from the casting's lack of a feeder and grew outward from the defect. The slight shrinkage has drawn back the remaining liquid. In the worst-case scenario, shrinkage porosity could happen when the remaining solidifying liquid is moved from the casting into

the feeding system. A multitude of patterns, including centerline porosity, sponge porosity, layer porosity, surface-initiated porosity, and external shrinkage porosity, can be indicative of shrinkage porosity [9].

In a skin-freezing alloy that has not gotten enough liquid from the feeder, centerline porosity forms. The pore must run parallel to the casting's thermal axis in order to comply with geometry. The long-freezing-range alloy's sponge porosity developed with a suitable temperature gradient but insufficient feeder feed liquid. Insufficient inter-dendritic feeding in a low temperature gradient result in layer porosity. The liquid metal is dirty, as indicated by the formation of internal porosity [10]. Geometry dictates that the pores must be at right angles to the axis of the casting. When there was no liquid available from the feeder but the melt was clean, surface sink (also known as external shrinkage porosity) formed, leading to good, solid feeding. The sink is typically found on the casting's cope surface due to gravity. All of this can be measured by microstructure indicator.

The porosity caused by shrinkage can be measured generally using the alloy microstructure as a guide. When comparing, if the microstructure dimension is smaller, there will be a lower likelihood of porosity, which is a sign of shrinkage. The cooling rate can be linked to a smaller microstructure. If the microstructure can have a smaller size, the cooling rate can be faster. Prior to the metal casting session, the volume to area (V/A) ratio can be calculated to estimate the cooling rate. Theoretically, the cooling rate is faster if the V/A ratio is lesser. As a result of having less time to grow, the grain size seen in the microstructure is smaller.

So, this study aims to explore the relationship between microstructure and, of course, internal shrinkage, and the volume to area (V/A) ratio. When the V/A ratio is higher than it is lower, a smaller microstructure dimension—specifically, the grain size—is anticipated. Porosity and shrinkage will be reduced in proportion to the grain size. The properties of the casting alloy will most likely be impacted by shrinkage. Understanding the connection between the porosity/shrinking distribution of the aluminum alloy and the microstructural inhomogeneity of the casting is the goal. The emphasis is seen as important since the properties of the alloy are directly influenced by the microstructure, especially the grain structure.

2. Methodology

The current study was carried out in an induction furnace with a 50 kg holding capacity, 200 kW of power, and a frequency range of 1000–3000 Hz. The following materials were heated to a melting condition (aluminum alloy with 8% silicon). Subsequently, the molten metal was degassed and fluxed in order to reduce the chances of gas buildup and oxidation (Figure 1). Meanwhile, bentonite, water, and silica sand were combined to create a green sand mold. Before the melt was poured into a mold, it was cleaned and heated to 670$\pm$20^{o}C. The pattern was prepared as shown in Figure 2. To obtain microstructural specimens, test specimens (point location 1 to 5 from edge to center back to edge 30mm distance) were sectioned, ground, and polished using 0.3 µm alumina powder following solidification. The second set of sample coupons was trimmed to measure 15.0 x 15.0 x 2.0 mm. They were polished with 1.0 µm diamond paste after being mechanically ground to 2400 mesh on SiC paper. After polishing the samples to a mirror shine, ethanol and acetone were cleaned using ultrasonic agitation for ten minutes. Before being exposed, the samples were dried and kept in a desiccator. After the specimens' microstructure was characterized using scanning electron microscopy (SEM), X-ray energy dispersive spectroscopy (EDS) was used to analyze their chemical compositions. A hardness test and an optical microscope were then used to visualize the test samples.

Fig. 1. Experimental setup during molten metal pouring

Fig. 2. Pattern for experimental setup

3. Results

3.1 Microstructure Evaluation

An alloy with a eutectic composition, consisting of different component alloys containing silicon, aluminum, and other elements, was produced during the casting process. Among the processes involved in solidification were phase formation, element solubility, and segregation. The composition of this alloyed aluminum varies based on the solubility of the individual elements. An analysis was conducted on the correlation between the average grain size and the microstructure at the big end (the area between the sprue), middle, and small ends of the pump coupling (the portion that connects to the green sand mold). The grain size decreases in the outer space (close to the mould wall), increases in the casting cavity's center, and then decreases once more at the right end as shown in Figure 4 to 8. The main cause of it is the molten aluminum alloy at the pump coupling part's edge cooling quickly. The molten heat can escape more easily in the direction of the green sand mold.

As a result, heat movement between different temperatures gradient is faster. The microstructure in the form of shape factor and the cooling rate are proportionate, and vice versa. This happens as a result of the homogeneous heat transmission from the grain to its surroundings

reflecting the rapid cooling. All of the heat is extracted from the grain in the same direction and at the same rate if the pace is faster. Therefore, once heat transfer is stopped, the same direction will reflect to a nodule or spherical shape that converges or convexes. The shape factor equal to one is the definition of a perfect circle. A value near 1 (spherical shape) usually indicates better mechanical properties [11].

Grain size is largely determined by the number of nuclei in the interim. All of this takes place in the nucleation stages. Grain size will start to increase once the total number of nuclei has been determined. Grain size will therefore increase as the number of nuclei generated decreases. Conversely, the smaller the particle size, the more nuclei formed. Growth rate decreases as cooling rate rises because slower growth kinetics are the result [12]. This theory clarified why fine grit formed after faster cooling rate. Furthermore, the grain has enough time to enlarge and produce growth that outpaces the quick cooling rate when the cooling rate drops. Consequently, samples that cool more slowly have larger grains than samples that cool more quickly [13].

From the pump coupling's big end (less V/A) to its middle sections (more V/A), the grain size increases gradually. The grain size was then shown to decrease from the middle (more V/A) to the small end (less V/A). It is evident that as the V/A casting cavity ratio increases from smaller to larger, the rate of cooling increases as well as shown in Figure 9. The reason for this is that the smaller V/A portion had less time to grow in comparison [14].

Furthermore, the size of the grain size affects the microhardness value as shown in Table 1. Higher values of hardness and strength are correlated with smaller grain sizes, and this relationship was observed in the sample taken when the V/A value was lower [15]. Thus, it can be said that the V/A has a significant impact on component strength and should be carefully taken into account when designing risers and gates [16].

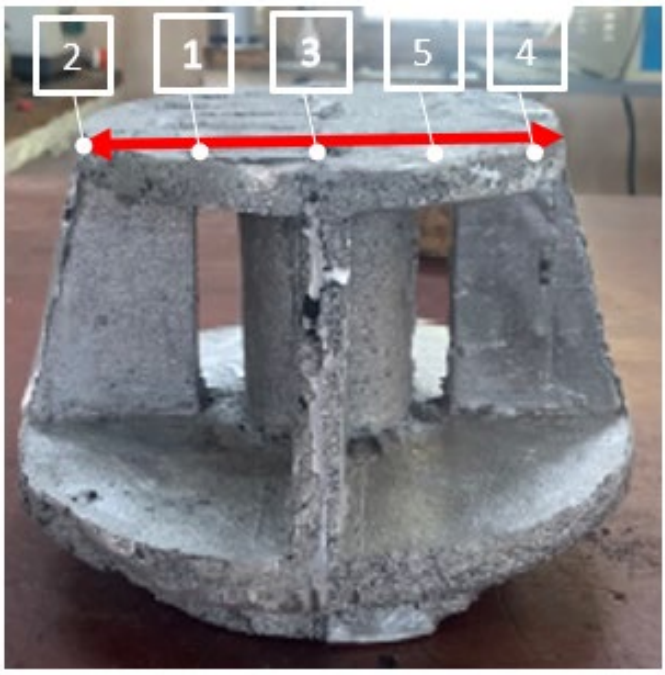

Fig. 3. Point location inspected due to V/A ratio on casting cavity

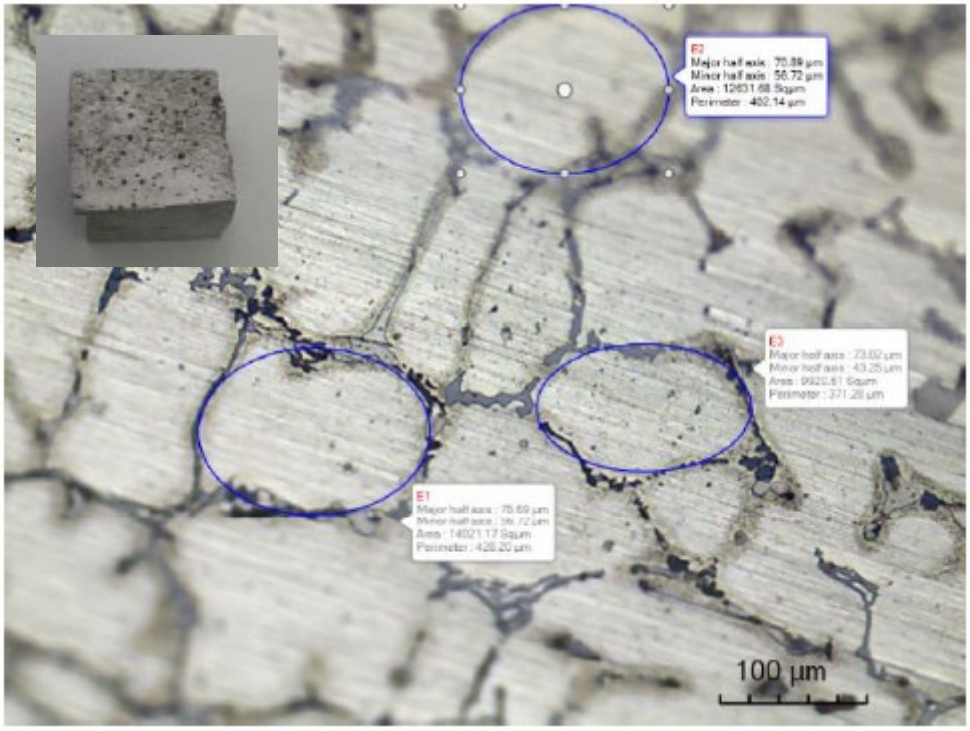

Fig. 4. Microstructure's grain size at sample location 1

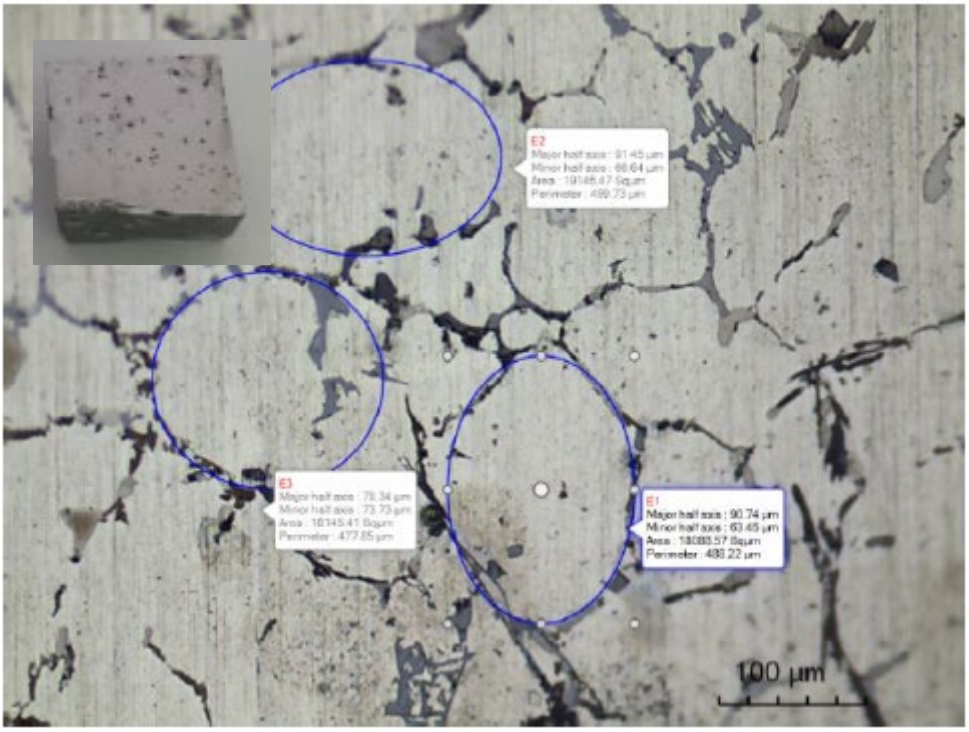

Fig. 5. Microstructure's grain size at sample location 2

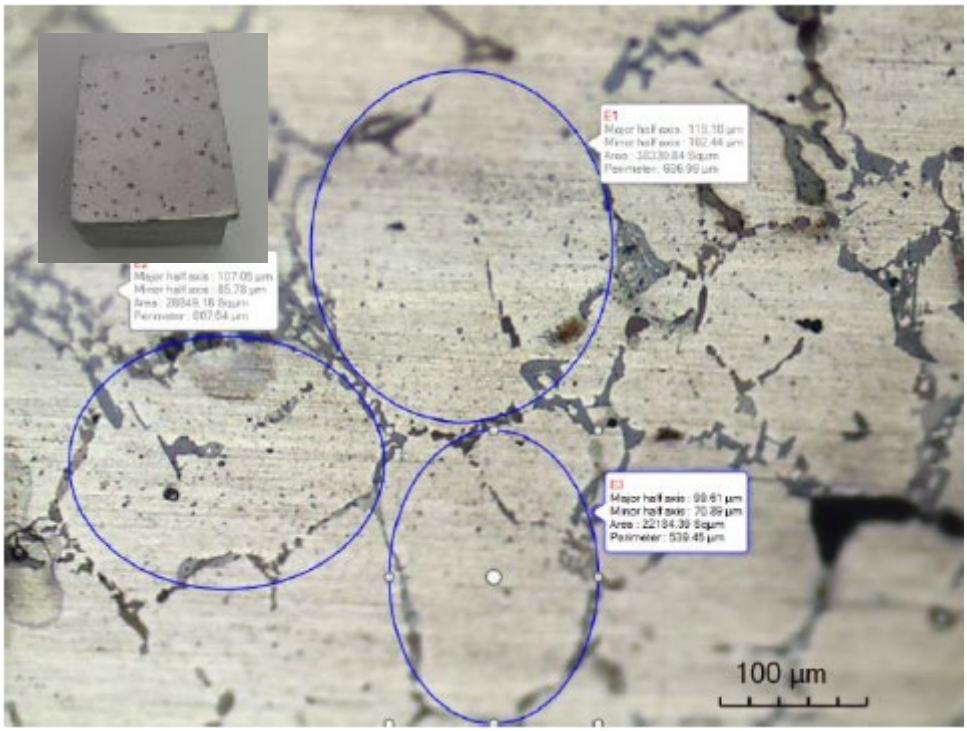

Fig. 6. Microstructure's grain size at sample location 3

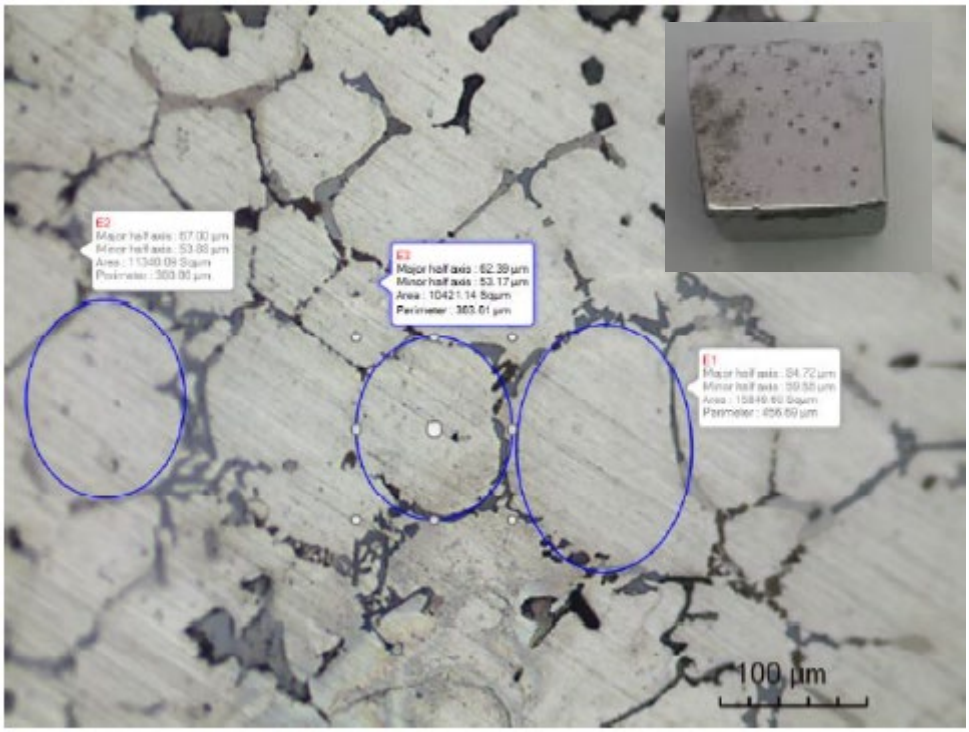

Fig. 7. Microstructure's grain size at sample location 4

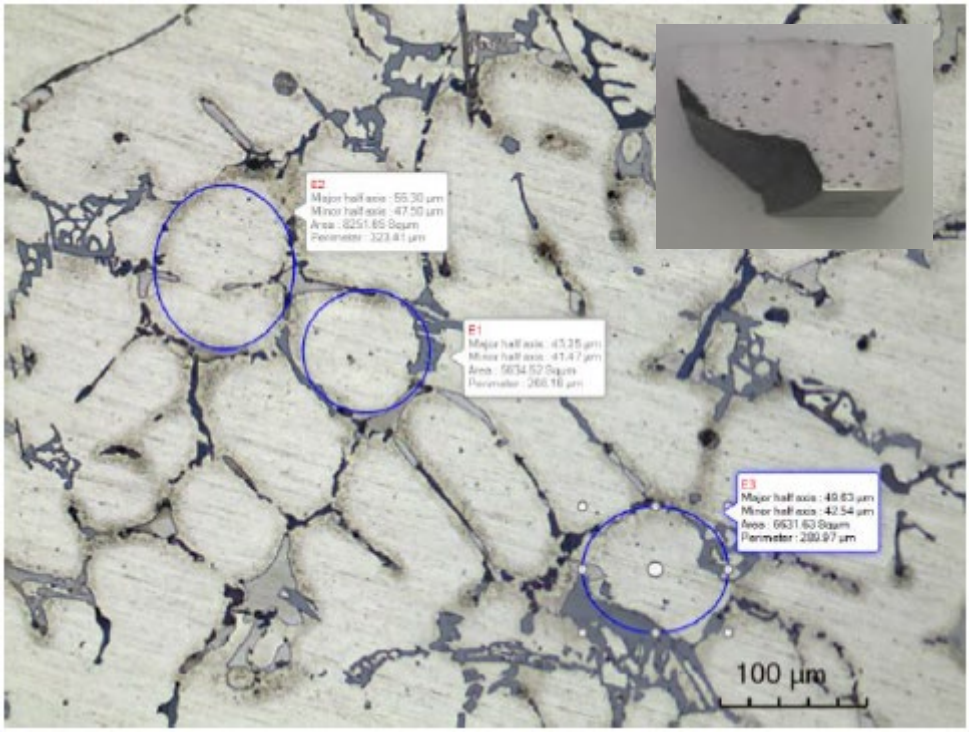

Fig. 8. Microstructure's grain size at sample location 5

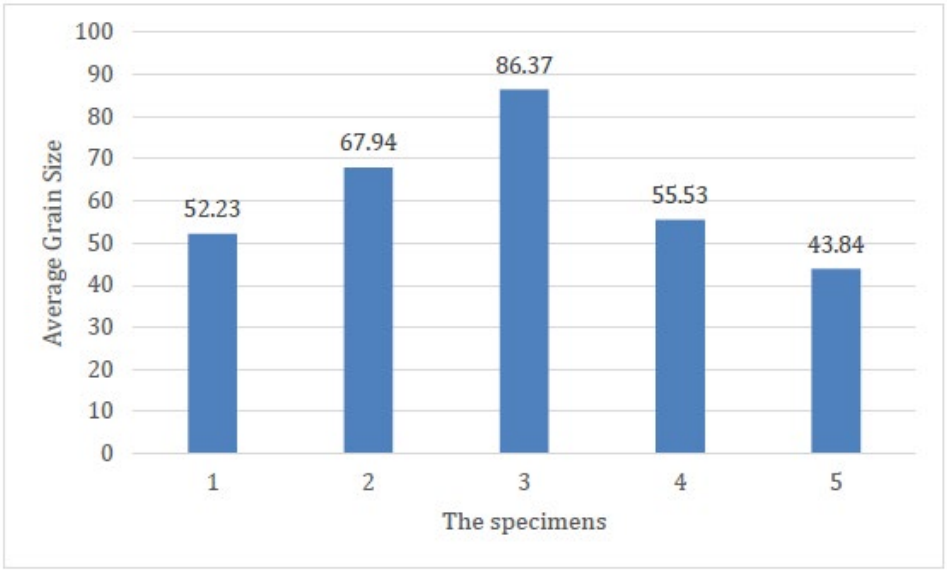

Fig. 9. Average grain size based on specimen's location

Table 1
Comparison of sample location on V/A ratio to grain size and size shape factor

Sample location	V/A ratio	Average grain size	Shape factor	Micro-hardness HV
1	1.1	52.23	0.7910	109.77
2	1.3	67.94	0.7964	104.12
3	1.6	86.37	0.8915	98.56
4	1.3	55.53	0.7897	104.57
5	1.1	43.84	0.7044	108.78

4. Conclusions

This paper discusses the evaluation of microstructure sizes and dimensions in an aluminum alloy which dimensioned as pump coupling components. Grain size did not follow a constant dimension; rather, it followed the volume to area ratio. The grain sizes are averaging larger at the higher V/A value, even though their patterns are almost identical. On the other hand, when the V/A value decreases, the grain size decreases. The majority of grain measurements showed up as 40–90 µm sizes. Around this grain structure were potential areas of porosity, void, and other segregation elements that became trapped during the solidification phase [17].

Acknowledgement

This research was funded by a grant from Ministry of Higher Education of Malaysia (FRGS Grant FRGS/1/2022/TK10/UMP/02/64 - RDU220135) and university's internal grant (RDU220305).

References

[1] Çelik, Gülşah Aktaş, Maria-Ioanna T. Tzini, Şeyda Polat, Ş. Hakan Atapek, and Gregory N. Haidemenopoulos. "Thermal and microstructural characterization of a novel ductile cast iron modified by aluminum addition." *International Journal of Minerals, Metallurgy and Materials* 27 (2020): 190-199. https://doi.org/10.1007/s12613-019-1876-8

[2] Martin, John. *Materials for engineering*. Woodhead Publishing, 2006.

[3] Ming, Li, Li Yuan-dong, Yang Wen-long, Zhang Yu, and Wang Zong-gang. "Effects of forming processes on microstructures and mechanical properties of A356 aluminum alloy prepared by self-inoculation method." *Materials Research* 22 (2019): e20180698. https://doi.org/10.1590/1980-5373-mr-2018-0698

[4] Benjunior, B., A. H. Ahmad, Maarof Mohd Rashidi, and M. S. Reza. "Effect of different cooling rates condition on thermal profile and microstructure of aluminium 6061." *Procedia engineering* 184 (2017): 298-305. https://doi.org/10.1016/j.proeng.2017.04.098

[5] Chen, Wen-Jong, Cai-Xuan Lin, Yan-Ting Chen, and Jia-Ru Lin. "Optimization design of a gating system for sand casting aluminium A356 using a Taguchi method and multi-objective culture-based QPSO algorithm." *Advances in Mechanical Engineering* 8, no. 4 (2016): 1687814016641293. https://doi.org/10.1177/1687814016641293

[6] Ingle, Vaibhav, and Madhukar Sorte. "Defects, root causes in casting process and their remedies." *Int. J. Eng. Res. Appl.* 7, no. 3 (2017): 47-54. https://doi.org/10.9790/9622-0703034754

[7] Salleh, M. S., N. N. M. Ishak, S. H. Yahaya, and A. Abdullah. "Effect of equal channel angular pressing on the microstructure and mechanical properties of a356 alloy." *Journal of Advanced Manufacturing Technology (JAMT)* 12, no. 2 (2018): 79-92.

[8] Santhi, Samavedam. "Calculation of Shrinkage of Sand Cast Aluminum Alloys." *Int. J. Appl. Eng. Res* 13, no. 11 (2018): 8889-8893.

[9] Davis, J. R. "Aluminum and Aluminum Alloy Castings." *Casting*, no.1 (2018): 1059–1084.

[10] El-Mahallawi, Iman Sallah-ElDeen, Tamer Samir Mahmoud, Ahmed Mohamed Gaafer, and Fouad Helmi Mahmoud. "Effect of pouring temperature and water cooling on the thixotropic semi-solid microstructure of A319 aluminium cast alloy." *Materials Research* 18 (2015): 170-176. https://doi.org/10.1590/1516-1439.304114

[11] Rashidi, M. M., and A. H. Ahmad. "Investigation of nickel aluminium bronze castings properties by degassing agent technique." In *IOP Conference Series: Materials Science and Engineering*, vol. 469, no. 1, p. 012037. IOP Publishing, 2019. https://doi.org/10.1088/1757-899X/469/1/012037

[12] Liang, Guofang, Yahia Ali, Guoqiang You, and Ming-Xing Zhang. "Effect of cooling rate on grain refinement of cast aluminium alloys." *Materialia* 3 (2018): 113-121. https://doi.org/10.1016/j.mtla.2018.08.008

[13] Shahria, Sumaiya, Md Tariquzzaman, Md Habibur Rahman, Md Al Amin, and Md Abdur Rahman. "Optimization of molding sand composition for casting Al alloy." *International Journal of Mechanical Engineering and Applications* 5, no. 3 (2017): 155-161. https://doi.org/10.11648/j.ijmea.20170503.13

[14] Khalajzadeh, Vahid, and Christoph Beckermann. "Simulation of shrinkage porosity formation during alloy solidification." *Metallurgical and Materials Transactions A* 51 (2020): 2239-2254. https://doi.org/10.1007/s11661-020-05699-z

[15] Kucharčík, L., M. Brůna, and A. Sládek. "Influence of Chemical Composition on Porosity in Aluminium Alloys." *Archives of Foundry Engineering* 14, no. 2 (2014): 5-8. https://doi.org/10.2478/afe-2014-0026

[16] Scharifi, Emad, Alexander Danilenko, Ursula Weidig, and Kurt Steinhoff. "Influence of plastic deformation gradients at room temperature on precipitation kinetics and mechanical properties of high-strength aluminum alloys." *J. Eng. Res. Appl* 9, no. 1 (2019): 24-29.
[17] Shahria, Sumaiya, Md Tariquzzaman, Md Habibur Rahman, Md Al Amin, and Md Abdur Rahman. "Optimization of molding sand composition for casting Al alloy." *International Journal of Mechanical Engineering and Applications* 5, no. 3 (2017): 155-161. https://doi.org/10.11648/j.ijmea.20170503.13